

Supramolecular evolution over an initial period of biodegradation of lactide and caprolactone based medical (co)polyesters

*Jone M. Ugartemendia, A. Larrañaga, H. Amestoy, J. R. Sarasua**

University of the Basque Country (UPV-EHU) Department of Mining-Metallurgy Engineering and Materials Science, School of Engineering, Alameda Urquijo s/n, 48013 Bilbao, Spain.

Basque Excellence Research Center in Macromolecular Design & Engineering, POLYMAT, P^o Manuel de Lardizabal 3, 20009 Donostia-San Sebastián, Spain.

*Corresponding author. Phone: +0034 946 014 271. Fax: +0034 946 014 180. E-mail: jr.sarasua@ehu.es

KEYWORDS

Poly lactide, poly(L-lactide-co- ϵ -caprolactone), physical aging, enthalpy relaxation, dynamic mechanical properties, TMDSC.

ABSTRACT

Phase-structural changes and enthalpic relaxation behavior of poly(D,L-lactide) (PDLLA), poly(L-lactide) (PLLA) and poly(L-lactide-co- ϵ -caprolactone) (PLCL) copolymers with a lactide molar content ~70 % and having different randomness character (PLCL_{r1}: R=0.69; PLCL_{r2}: R=0.92) were evaluated over 7 days in phosphate buffered saline (PBS) at 37 °C. Results obtained by Temperature Modulated Differential Scanning Calorimetry (TMDSC) and Dynamic

Mechanical Analysis (DMA) showed an increase in the value of enthalpic relaxation (δ) and the narrowing of the $\tan \delta$ peak, respectively, indicating the reduction in molecular mobility and a more uniform distribution of the entropic states as the aging time increased. The results obtained for PLCLs were clearly affected by chain microstructural magnitudes, l_{LA} (PLCL r_1 =4.35 and PLCL r_2 =3.45). Both showed a crystallization process accompanied by amorphous phase separation during the early stage in PBS. DSC and DMA results also revealed faster structural changes as a result of new supramolecular arrangements as well as a higher tendency to crystallize for PLCL r_1 regarding PLCL r_2 .

INTRODUCTION

The choice of an adequate medical implant made of bioresorbable polymeric biomaterials may require the understanding of the structural changes undergone during the biodegradation process, or even during the storage time, leading to physical and mechanical properties changes over time. Time-dependent changes in structure and properties are well known consequences of physical aging. This phenomenon is quite common in polymers that are in thermodynamically unstable state after transformation by hot melt processes. On cooling thermodynamical properties resulting from the first derivative of the Gibb's energy over temperature, for example, specific volume (V), enthalpy (H) and entropy (S) undergo a change of slope around the glass transition temperature (Figure 1). After solidification thermodynamically more stable states will be prompted by additional isothermal annealing conditions conducted at temperatures below the glass transition temperature ($T_a < T_g$). This will enable a material for a more close-to- equilibrium state through localized dynamics of conformational chain motions involving time and temperature. In this work, the relaxation behavior is studied in terms of the reduction in the excess volume and excess enthalpy T_a [1] leading to a less entropic new metastable equilibrium.

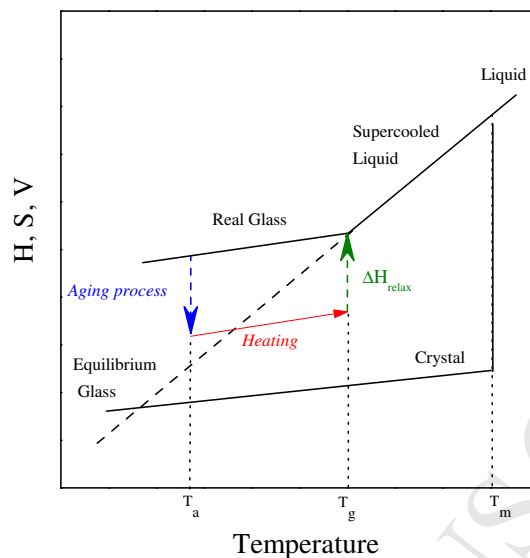


Figure 1. Schematic illustration of changes in enthalpy (H), entropy (S), and volume (V) as a function of temperature during the aging process.

The excess enthalpy due to physical aging is recovered in the T_g region when the aged polymer is heated. Therefore, discrete values of the enthalpy loss or enthalpy relaxation (δ) on annealing at T_a could be inferred from Differential Scanning Calorimetry (DSC) scans at a constant heating rate. For aged samples, the extra energy required for glass transition brings about an increase in the area of the endothermic peak in the vicinity of T_g . However, the signals related to both processes, the change in specific heat capacity (C_p) and the relaxation enthalpy cannot be evaluated individually by DSC because when two or more transitions occur simultaneously, it may be impossible to interpret the DSC results. A temperature modulated DSC, TMDSC [2-4], is a useful technique to solve this problem. With this technique, the individual components of the total heat flow, the capacity component, known as reversing heat flow, and the kinetic

component, known as nonreversing heat flow, can be determined separately: ΔC_p may be obtained from the reversing signal and the δ from the nonreversing signal, sometimes named as reversing C_p and nonreversing C_p , respectively [5].

The term physical aging has also been widely used to denote the evolution during storage time that lead to crystallization, this causes a change in the mechanical properties, making the polymeric material more brittle [6, 7]. This is the well-known case of polyethylene, for example [8-10]. During aging, the molecular mobility is often sufficient to allow molecular segments in the amorphous phase to progressively realign and crystallize, either in the form of new crystals between the pre-existing lamellar crystals, or by adding newly formed crystals to pre-existing ones, having as a result an increase in crystallinity fraction.

The effect of physical aging on PLAs has been previously discussed in literature [11-13]. Pengju Pan and co-workers analyzed the conformational features of PLLA during aging and the effect of that process on the microstructure and molecular dynamics of PLLA. By means of FTIR and solid-state NMR spectroscopy, they found that during aging the *gg* conformers rearrange into more energy-favorable *gt* counterparts [14]. Microstructural rearrangements taking place during the aging process were also considered responsible for the enhanced crystallization and consequently for the embrittlement of PLLA [15, 16]. A few works can be also found about physical aging on PLCL copolymers yet involving long aging times [17-19].

If changes related to the physical aging process stem from segmental mobility, it is reasonable to assume that chain microstructure features (composition and randomness character of comonomer repeat units) will have a profound effect on the final supramolecular structure and thus on properties. In this work, polymers having the same nature but different structure of the polymeric

chain are studied. On the one hand, the behavior of poly(L-lactide) (PLLA) and poly(DL-lactide) (PDLLA) will be compared and on the other hand, two poly (L-lactide- ϵ -caprolactone) copolymers of similar composition but different block lengths are object of this work. Proper correlations of polymer molecular characteristics with their resulting structure and properties will be studied during an initial period of 7 days in PBS by means of DSC, TMDSC, AFM and dynamic mechanical analysis (DMA) after 1, 3 and 7 days.

MATERIALS AND METHODS

Table 1 shows the main specifications of the commercial polymers and copolymers employed in this work. The weight average molecular weight (M_w) and the polydispersity index, $D = M_w/M_n$ of the studied polymers were determined by Gel Permeation Chromatography calibrated to PS standards, chloroform as an eluent, with a Waters 1515 chromatograph device equipped with a Waters 2414 refractive index (RI) detector. On the other hand, the composition (%LA), the microstructural magnitudes (l_i) and the randomness character (R) of the PLCL copolymers were determined in a previous work by ^1H and ^{13}C Nuclear Magnetic Resonance spectroscopy and are summarized in Table 1 [20]. The main difference between PLCL_{r_1} and PLCL_{r_2} is essentially the lactide average sequence length (l_{LA}) and the randomness character (R). The PLCL_{r_2} copolymer has shorter l_{LA} and a more random character, 3.45 and 0.92, respectively, in contrast to 4.35 and 0.69 for PLCL_{r_1} .

Table 1. Specifications of the materials. M_w : weight average molecular weight; D: polydispersity index; %LA: lactide molar content; l_{LA} : lactide average sequence length; R: randomness character (considering that in a diblock copolymer $R \rightarrow 0$ while in a random one $R \rightarrow 1$).

	PLLA	PDLLA	PLCL r_1	PLCL r_2
M_w (g mol $^{-1}$)	130x10 3	127x10 3	136x10 3	185x10 3
D	1.66	1.92	1.68	1.71
%LA	-	-	67.1	70.0
l_{LA}	-	-	4.35	3.45
l_{CL}			2.13	1.54
R	-	-	0.69	0.92
Provider	Biomer	Purac	Purac	Purac

For this work polymer sheets of ~1 mm thickness were prepared by compression moulding in a Collin's P200E hydraulic press at 200 °C and 240 bar followed by water quenching in order to guarantee an amorphous state. From these sheets, samples 20 mm long and 4 mm wide were obtained. Each sample was submerged in 15 ml of phosphate buffered saline (PBS) and stored in an oven at 37 °C for 7 days. At different periods of time (1, 3 and 7 days) 3 samples of each polymer were removed from the PBS and vacuum-dried. Non-submerged samples (day 0) were employed as a reference.

Standard and temperature modulated dynamic scanning calorimetries (DSC and TMDSC) were carried out on a DSC 2920 (TA Instruments). For standard DSC, samples (6-8 mg) were heated from -85 to 220 °C at 20 °C min⁻¹. This scan was employed to determine the cold crystallization temperature (T_c), the crystallization enthalpy (ΔH_c), the melting temperature (T_m) and the heat of fusion (ΔH_m) of all the samples, as well as the glass transition temperatures (T_g) of the PLCL r_1 and PLCL r_2 copolymers. The determination of T_g and enthalpic relaxation (δ) for PLLA and PDLA was measured by means of TMDSC with a modulation amplitude of 0.75 °C over a period of 120 s. The heating scan was carried out from 20 °C to 75 °C at a heating rate of 0.5 °C min⁻¹ and the sample weight was 4-6 mg in all cases. To correct the frequency effect, after the heating process above T_g , the sample was cooled under the same TMDSC conditions as used for heating. Any peak area in the nonreversing signal on cooling can only be caused by the frequency effect. This area was subtracted from the peak area obtained on heating so as to calculate the peak area which was just due to enthalpic recovery.

Dynamic mechanical measurements were carried out using a DMA/SDTA861e (Mettler Toledo) in tensile mode. The PDLA and PLLA samples were heated from 20 to 100 °C at a heating rate of 3 °C min⁻¹, a frequency of 1 Hz and the displacement and force amplitude were maintained at 25 μ m and 0.5 N, respectively. The PLCL r_1 and PLCL r_2 samples were heated from -20 to 100 °C at a heating rate of 3 °C min⁻¹, a frequency of 1 Hz and the displacement and force amplitude were maintained at 30 μ m and 3 N, respectively.

AFM imaging of the PLCL r_1 copolymer sample was carried out with a Nanoscope III Multimode scanning probe microscope (Bruker) with a scanner whose maximum range was between 100 and 10 μ m in xy and z directions, respectively. Samples were prepared by depositing a few drops of the polymer solution (3 wv.%) onto a mica substrate and then spin coated. The specimen was

subjected to melt-quenching prior to submerging it in PBS at 37 °C for one day. All imaging was conducted in tapping mode using standard silicon cantilever with a resonance frequency between 254-321 KHz and spring constant of 20-80 N m⁻¹.

RESULTS AND DISCUSSION

Physical aging during an initial stage of biodegradation in PBS of PLLA and PDLLA

DSC heating scans for PLLA and PDLLA samples submerged in PBS over 0, 1, 3 and 7 days at 37 °C are shown in Figure 2. Since both PLLA and PDLLA were submerged at a temperature below their T_g , they underwent a physical aging process during the course of the experiment. PLLA samples displayed the usual behavior of semicrystalline polymers; with a glass transition temperature followed by a cold crystallization process and melting of the developed crystals. On day 0, just after quenching the sample, the thermogram presented a T_g at ~60 °C and small cold crystallization and melting peaks at ~117 °C and ~170 °C, respectively. However, after only 1 day submerged in PBS, PLLA displayed an endothermic peak at its T_g and both the cold crystallization (ΔH_c) and melting (ΔH_m) enthalpies increased considerably. The endothermic peak at T_g , is related to the recovery of the excess of enthalpy that polymers acquire on quenching from the melt. Although no significant changes are observed in the DSC traces for PLLA in the T_g values, the effect of aging on the cold crystallization behavior is evident. In this sense, as shown in Table 2, the ΔH_c rises from 9.8 J g⁻¹ to 40.0 J g⁻¹ on the first day. For longer aging times, few changes were observed in the DSC scans.

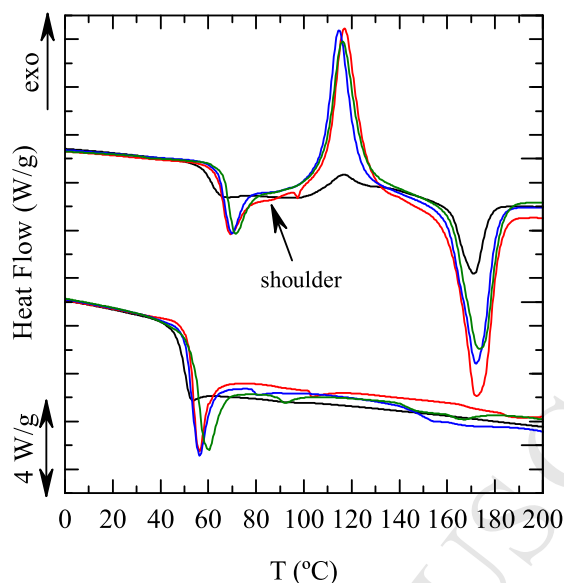


Figure 2. First DSC scans for PLLA (above) and PDLLA (below) samples submerged in PBS at 37°C during 0 (black), 1 (red), 3 (blue) and 7 (green) days.

The effect of aging on cold crystallization behavior has been already reported for PLLA in literature [16, 21]. This change in the cold crystallization peak can be explained in terms of chain rearrangements. Just after quenching, polymer chains are disordered with many conformational states in a non-equilibrium state. Conformational defects such as entanglements or chain torsions make the nucleation and the subsequent diffusion of polymer chains less probable, impeding the crystallization process. However, during aging, the chain conformation and microstructure readjust to a more organized and more packed chain structure in order to drive the material closer to equilibrium or to the more energy-favorable state. Local ordering domains formed during aging could act as nucleation precursors in the subsequent crystallization process. This is the reason why the crystallization process becomes more prevalent with aging. In spite of the

increase in both ΔH_m and ΔH_c during aging, the neat enthalpy ($\Delta H_m - \Delta H_c$) stays almost constant, near zero, during the study, indicating that the polymer obtained is essentially amorphous and no new crystals developed during the aging treatment.

Table 2. Thermal properties of PLLA and PDLLA after conformation by melt-quenching (0 day) in water and after being submerged in PBS over 1, 3 and 7 days. T_g : glass transition temperature, T_p : maximum of the relaxation enthalpy peak and δ : relaxation enthalpy; were obtained by TMDSC and T_c : cold crystallization temperature, ΔH_c : crystallization enthalpy, T_m : melting temperature and ΔH_m : melting enthalpy, were obtained by conventional DSC.

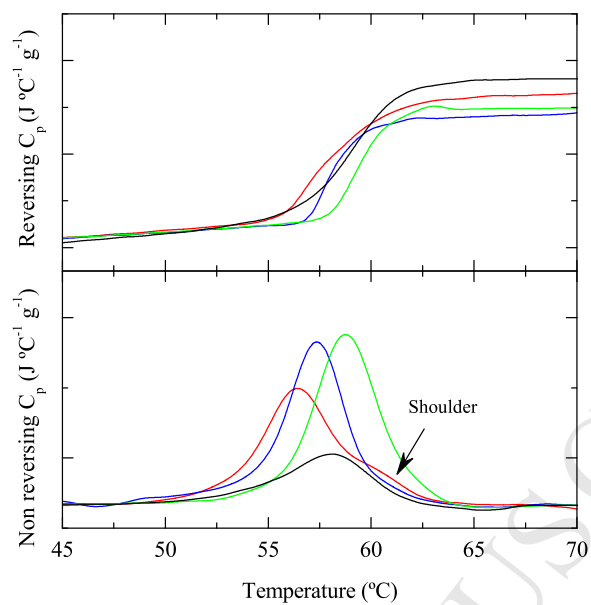
	t_a (days)	TMDSC			DSC			
		T_g (°C)	T_p (°C)	δ (J g ⁻¹)	T_c (°C)	ΔH_c (J g ⁻¹)	T_m (°C)	ΔH_m (J g ⁻¹)
PLLA	0	59.1	58.1	1.6	116.8	9.8	171.0	14.9
	1	56.9	56.4	4.2	116.8	40.0	172.1	43.2
	3	57.7	57.4	4.5	114.7	42.1	172.1	46.6
	7	59.1	58.8	5.3	116.2	41.6	173.6	42.4
PDLLA	0	46.0	45.0	1.0	-	-	-	-
	1	45.9	44.6	1.5	-	-	-	-
	3	44.6	44.0	1.4	-	-	-	-
	7	44.7	44.4	2.0	-	-	-	-

In contrast to PLLA a unique transition, T_g , is observed for PDLLA, Figure 2, in agreement with its amorphous nature. The appearance of an enthalpic relaxation peak is the only difference

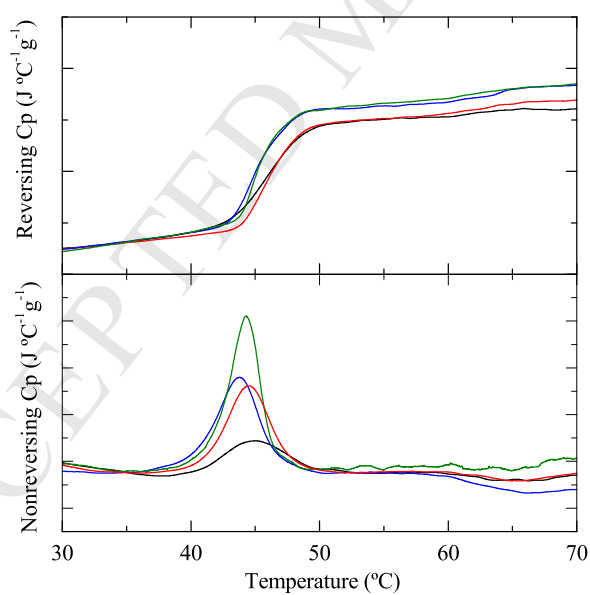
observed between samples submerged on different days. As for the PLLA sample, the main change in the area of the endothermic peak is observed on the first day and then it stays almost constant. Referring to the DSC traces for PDLLA, it seems that the relaxation peak in the sample aged for 7 days shifts to higher temperatures when compared to the other aged samples.

Interestingly, for the PLLA samples aged 1 day, a shoulder was discernible at the high-temperature side of the relaxation endothermic peak. However, this shoulder was not detected for the aged PDLLA samples, as can be observed in Figure 2. The same behavior has been reported by Pengju Pan et. al. for PLLA and PDLLA annealed at 40 °C for aging times between 3-24 h [15]. The lower temperature side peak is believed to correspond to the segmental dynamic in the bulklike phase, whereas the higher temperature one to the constrained motion in the amorphous phase located within the crystalline phase. The main consequence of this immobilization is that more temperature is needed for the transition, thus, the T_g is extended towards the high temperature side [22-24]. The shoulder detected in our sample is much smaller compared to the lower temperature one, indicating that the fraction of the constrained amorphous phase in the sample is insignificant. Therefore, it may be concluded that the content of the crystalline phase in the sample is extremely small, as observed in the values of neat enthalpy illustrated in Table 2.

However, for the two polymers, PLLA and PDLLA, the apparent C_p observed in the DSC traces for each aged sample results from an overlapping enthalpy relaxation, δ , and C_p of the glass transition. Therefore, in order to assess enthalpic recovery, it is necessary to separate the change in heat capacity at T_g from the endothermic peak caused by the enthalpic recovery process. This is not possible with the standard DSC and so TMDSC is required. With this technique, the change in heat capacity occurs in reversing signal while enthalpic recovery, which is a kinetic process, occurs in the nonreversing signal [5].



(a)



(b)

Figure 3. Reversing (above) and Nonreversing C_p (below) of (a) PLLA and (b) PDLLA after being submerged in PBS at 37 °C during 0 (black), 1 (red), 3 (blue) and 7 (green) days.

Parts (a) and (b) in Figure 3 display the TMDSC results as reversing and nonreversing C_p for PLLA and PDLLA, respectively. The change in real heat capacity and its associated T_g is studied by analyzing the results obtained from the reversing signal, while the enthalpic recovery, δ , and the maximum of the relaxation enthalpy peak (T_p) were evaluated in the nonreversing signal. The enthalpy relaxation was determined as the integral of nonreversing C_p in Figure 3. Table 2 summarizes the values calculated by analyzing TMDSC signals of T_g , T_p , δ .

For PLLA, T_p shifted slightly to higher temperatures, while the value of δ rapidly increased at short t_a and then slowed down at longer t_a . It increases from 1.6 J g^{-1} to 4.2 J g^{-1} on the first day and then slows to reach a value of 5.3 J g^{-1} at the end of the study (day 7) (see Table 2). This behavior is in agreement with the results reported by Kwon and coworkers [13] for polylactide films containing various D-isomer contents as a function of T_a . They found similar exponential tendencies in δ against t_a for all the polylactide samples tested. This behavior can easily be explained if it is considered that the thermodynamic driving force decreases when the polymer chains are closer to attaining the equilibrium state. Hence, the kinetics by which polymer chains approach a more favorable state becomes slower with t_a .

It is worth mentioning the shoulder detected in the nonreversing C_p signal for the PLLA sample submerged in PBS for 1 day. This result provides a record of the existence of different relaxation modes, the first one ascribed to the undisturbed amorphous region and the second one to the constrained amorphous region with reduced mobility. In this case the results obtained from both, DSC and TMDSC, are in total agreement.

T_g derived from reversing C_p also shifted to higher temperatures for PLLA after aging as illustrated in Figure 3 and Table 2. Although the difference between T_g for 1-7 days is just $2 \text{ }^\circ\text{C}$,

differences in the shapes of reversing C_p are significant. At larger aging times, the transitions became narrower and steeper due to different packing parameters. As aging proceeds, the formation of a more ordered packing of polymer chains makes, on the one hand, the overall entropic state of the system decrease and on the other hand, narrows the distribution of the different entropic states. Therefore, changes in the heat capacity from glass to liquid, i.e changes with temperature in reversing C_p , occur at higher temperatures and in a narrower temperature range because the entropic distribution of the system is more uniform.

Table 3. Molecular weight of PLLA and PDLLA samples before and after being submerged for 7 days in PBS at 37 °C.

Material	t_a (days)	M_w (g mol ⁻¹)	M_n (g mol ⁻¹)	D
PLLA	0	130000	78000	1.66
	7	120000	70600	1.70
PDLLA	0	127000	66300	1.92
	7	86400	41400	2.09

For PDLLA, the value of δ suffered minor changes and a clear trend for T_p was not observed. Furthermore, the reversing C_p did not show the same trend as was observed for PLLA. The T_g seems to shift to a lower temperature and a slight broadening of reversing C_p signal can be

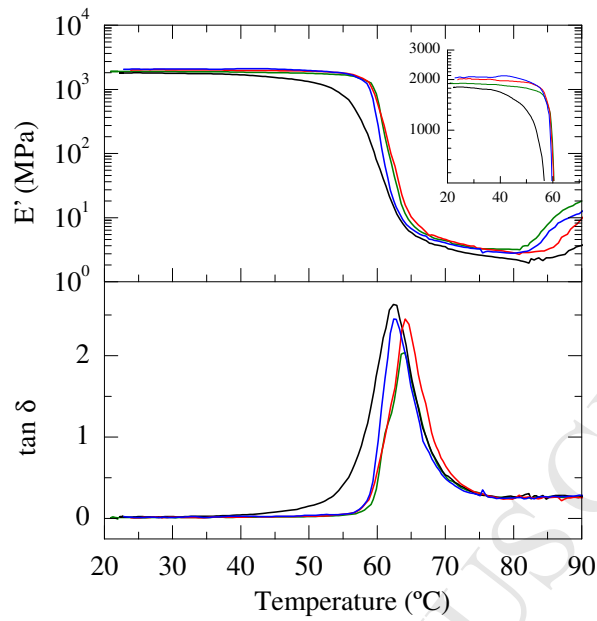
appreciated with t_a . These results suggest that another process besides aging is interfering with the PDLLA samples. The decrease in T_g , T_p , and the change in shape of reversing C_p towards a broader signal, could be indicative of molecular weight loss during the aging process in PBS. The molecular weights of PLLA and PDLLA samples were measured before (0 day) and after being submerged for 7 days in PBS at 37 °C. The results are shown in Table 3. In contrast to PLLA, which only lost 8 % of its initial molecular weight, the molecular weight for PDLLA dropped from 127×10^3 to 86.4×10^3 g mol⁻¹, that means a loss of 32 % during the period of the study. This drop in M_w might be enough to alter the behavior of the samples. Consequently, the combination of both effects (loss in molecular weight and aging) makes the interpretation of the results obtained for PDLLA difficult. In order to better understand the real state of the PDLLA samples a more thorough study is required.

The effect of aging was also analyzed using dynamic mechanical measurements. The temperature dependent curves of storage modulus (E') and $\tan \delta$ for PLLA and PDLLA after being submerged at 37 °C for 0, 1, 3 and 7 days are presented in Figure 4. Table 4 summarizes the temperature and values of $\tan \delta$ ($T_{\tan \delta}$ and $\tan \delta$), and the temperature of E' onset ($T_{E' \text{ onset}}$). The T_g was taken as the temperature of $\tan \delta$ and the $T_{E' \text{ onset}}$ was calculated as the temperature where the initial value of E' departs from linearity.

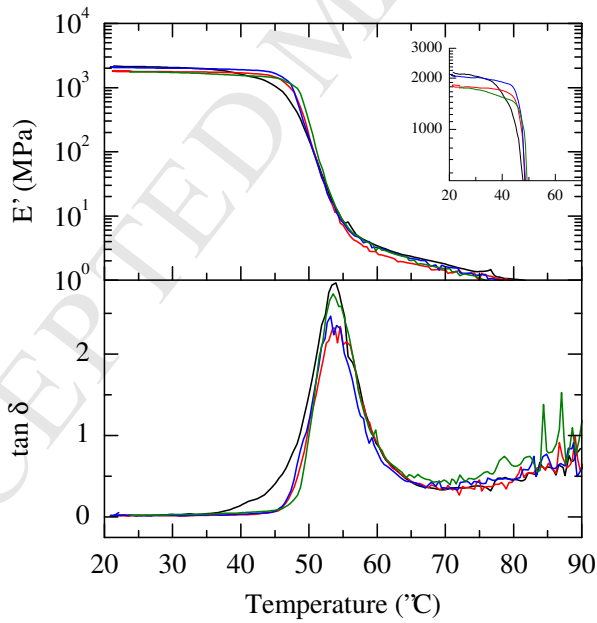
Although no significant changes are found in the $\tan \delta$ value for PLLA, the width of the $\tan \delta$ peak becomes narrower with aging, as shown in Figure 4 (a). The small shift in $\tan \delta$ to higher temperatures is consistent with the minor changes found in the TMDSC data in the T_g values (see Table 2). It can easily be seen by comparing the E' curves of the 0 day (unaged) and 1 day (aged) samples that $T_{E' \text{ onset}}$ for the latter is higher and the E' drop is steeper. The $T_{E' \text{ onset}}$ rises ~ 7 °C after being treated for only one day. Both results, the narrowing of the $\tan \delta$ peak and the more abrupt

drop in E' with temperature, account for the change in entropic states towards a narrower distribution with t_a , which is consistent with the behavior observed in the reversing C_p for PLLA.

On the other hand, a significant increase in the E' curves appeared around 80 °C for all PLLA samples. This is related to the cold crystallization occurring around this temperature during heating, as was demonstrated in the DSC traces in Figure 2. DMA curves prove that the increase in E' is higher with increasing t_a , indicating that the samples aged for longer times are more prone to the cold crystallization process upon heating. Moreover, the starting point at which the increase in E' occurs is shifted to lower temperatures for samples aged over longer periods. This means that cold crystallization occurs at lower temperatures in samples with a more ordered initial state than in samples with more defects, such as entanglements or chain torsion. Therefore, in view of the DSC and DMA results, it can be concluded that aging may be a precursor of the cold crystallization process.



(a)



(b)

Figure 4. Storage modulus (above) and $\tan \delta$ (below) of (a) PLLA and (b) PDLLA after being submerged in PBS at 37 °C during 0 (black), 1 (red), 3 (blue) and 7 (green) days.

Table 4. DMA properties of PLLA and PDLLA after conformation by melt-quenching (0 day) in water and after being submerged in PBS during 1, 3 and 7 days. $T_{\tan\delta}$: temperature at which $\tan\delta$ is maximum; $\tan\delta$: value of the $\tan\delta$ peak and $T_{E' \text{ onset}}$: the temperature where the initial value of E' departs from linearity.

	t_a (days)	$T_{\tan\delta}$ (°C)	$\tan\delta$ (value)	$T_{E' \text{ onset}}$ (°C)
<i>PLLA</i>	0	62.40	2.63	42.69
	1	64.11	2.45	49.80
	3	62.43	2.45	50
	7	64.07	2.03	48.07
<i>PDLLA</i>	0	54	2.87	35.8
	1	54.60	2.34	41.46
	3	53.63	2.47	38.6
	7	53.50	2.74	41.36

As can be observed in Figure 4 (b), DMA curves for PDLLA show no major changes, in complete contrast to PLLA. The temperature at which $\tan\delta$ is maximum ($T_{\tan\delta}$) stays almost constant, corroborating the small change observed in the data determined by TMDSC. However, the trend of $\tan\delta$ curves, as well as that of E' , showing a similar behavior to that observed for PLLA. The width of $\tan\delta$ peaks for the samples submerged in PBS over 1, 3 and 7 days was narrower than that of the non-submerged (day 0) sample and the drop in E' became steeper, indicating that the molecular mobility distribution become narrower for the submerged samples.

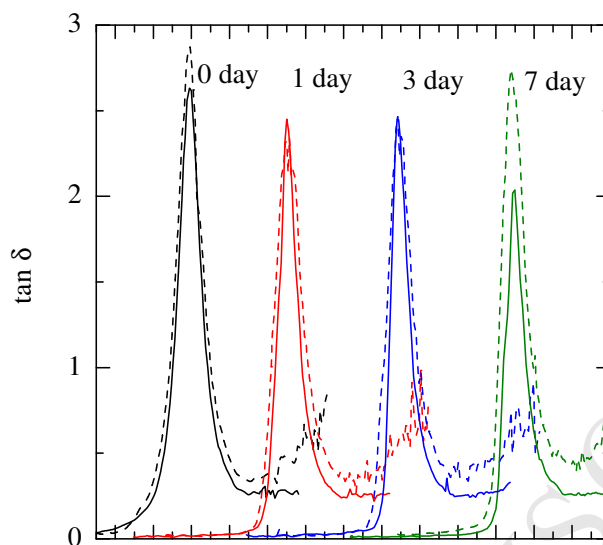


Figure 5. Comparison of the width of the $\tan \delta$ of PDLLA (dashed line) and PLLA (solid line) after being submerged in PBS at 37 °C during (black) 0 days, (red) 1 day, (blue) 3 days and (green) 7 days.

Tan δ curves of PLLA and PDLLA were also conveniently compared so as to analyze the effect of chain microstructure on chain rearrangement ability against aging time.

Figure 5 shows a qualitative comparison of the $\tan \delta$ for PLLA as a solid line and PDLLA as a dashed line for different aging times. In all cases, PLLA showed a narrower $\tan \delta$ peak, suggesting that at constant T_a and t_a chain reorganization towards a more densely packed structure is more easily achieved by PLLA than by PDLLA. That is to say, the presence of D-isomer in the chain architecture makes it more difficult for the polymer to undergo the relaxation process toward equilibrium. It is believed that polylactides with a lower D-isomer content have a higher potential to crystallize, i.e., polymer chains have more ability to pack in more ordered

domains, and thus can relax much efficiently at a given T_a , compared to polylactides with a higher D-isomer content [13]. Therefore, it stands to reason that the distribution of plausible different entropic states for PLLA at defined T_a and t_a is lower than for PDLLA, leading to a narrower $\tan \delta$ peak.

Physical aging during an initial stage of biodegradation in PBS of PLCL with different randomness character

In Figure 6, the first DSC scans for the PLCL r_1 sample submerged during 0, 1, 3 and 7 days in PBS are displayed. PLCL r_1 initially acted as a single phase amorphous copolymer showing a single hybrid T_g at ~ 22 °C, corresponding to an intermediate value between the T_g of PLLA (60 °C) and PCL (-60 °C). The single intermediate T_g value found for the quenched PLCL r_1 sample suggests the existence of a single miscible amorphous metastable phase, further corroborated by the intermediate $T_g=19$ °C value calculated from the Fox equation [25]. However, clear structural changes are observed when the copolymer is stored at 37 °C in PBS for 1 day. A double T_g behavior is visible and a melting peak appears around 128 °C. The first T_{g1} , would be associated with the hybrid amorphous miscible lactide-caprolactone (LA-CL) phase, whereas the second T_{g2} found around 61 °C, suggests the presence of phase separated amorphous polylactide domains.

Table 5. Thermal properties of PLCL_{r1} and PLCL_{r2} after conformation by melt-quenching (0 day) in water and after being submerged in PBS during 1, 3 and 7 days.

		T _{g1} (°C)	T _{g2} (°C)	T _m (°C)	ΔH _m (J g ⁻¹)
PLCL _{r1}	0	22.0	-	-	-
	1	15.2	61.0	128.4	11.4
	3	13.3	65.8	129.3	11.9
	7	13.1	69.6	130.5	12.3
PLCL _{r2}	0	21.8	-	-	-
	1	23.8	-	-	-
	3	17.6	64.7	91.1	a
	7	18.4	68.8	94.6	a

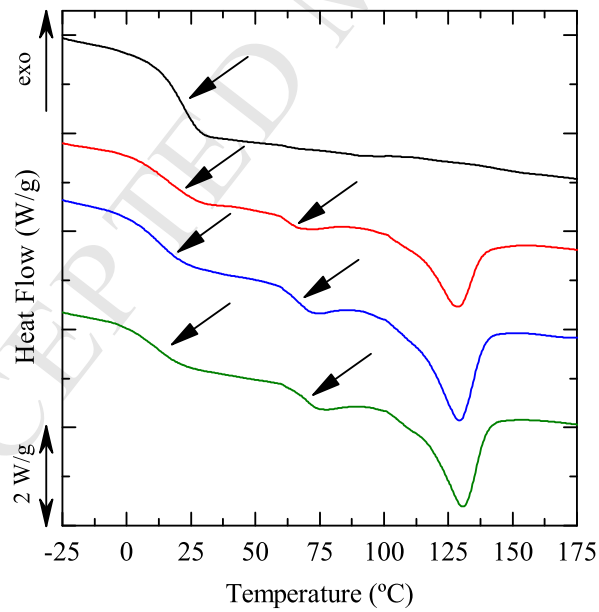


Figure 6. First DSC scans for PLCL_{r1} samples submerged in PBS at 37 °C during 0 (black), 1 (red), 3 (blue) and 7 (green) days.

The possibility of an endothermic signal at T_{g2} in aged PLCL, corresponding to a melting peak of polycaprolactone crystals is completely discarded. In a previous work [19] we demonstrated by WAXD that the aged PLCL presents diffraction peaks corresponding exclusively to the crystallization of α polylactide crystal, so ϵ -caprolactone building blocks do not crystallize during aging of PLCL. Note that the average sequence length of this statistical $PLCL_{r1}$ is very short ($l_{CL}=2.13$) for a 32.9 % molar composition of ϵ -caprolactone. In the above mentioned work, the WAXD results of PLLA, PCL and PLCL (non-aged and aged) were also included. Only an amorphous halo appears for as-quenched $PLCL_{r1}$ (non-aged) in contrast to well resolved diffraction peaks corresponding to PLLA and PCL homopolymers, revealing a completely amorphous phase structure in non-aged $PLCL_{r1}$ that evolves during aging until it is partly crystalline due to copolymer chains rearranging into polylactide α crystals. The diffraction peaks for aged $PLCL_{r1}$ can be unequivocally assigned to the α polymorph of polylactide. Therefore, the T_m registered in the first DSC scan corresponds to the melting of PLLA crystals.

The melting point depression for the $PLCL_{r1}$ copolymer in comparison to pure PLLA ($T_m=180$ °C) is explained by the diluting effect of ϵ -caprolactone units on a $PLCL_{r1}$ copolymer having a major presence of L-polylactide, which according to the experimental evidence provided here, has a large enough average length ($l_{LA}=4.35$) and L-lactide composition (67.1 %) to be capable of crystallization during aging. The endothermic peak at 128 °C is therefore the result of melting of α PLLA crystals developed during the aging period to which the PLCL copolymer is exposed to at 37 °C in PBS for 1 day. The ability of a PLCL to crystallize has been also reported by other authors [17, 18]. It was proved that the aging process enhances the crystallinity of amorphous

PLCL in the presence and absence of PBS, although more rapid changes were found for the samples in contact with PBS. It seems that the presence of plasticizing water accelerated the crystallization of the copolymer, probably because of the enhanced chain mobility.

Once the PLCL_{r1} is phase separated, as the time submerged in PBS increased, the T_{g1} slightly shifted to lower temperatures, from 22 °C, 0 day, to 13.1 °C after 7 days. This is due to the incorporation of some LA sequences of the LA-CL mixed phase to the polylactide crystalline domains. As this migration occurs, the hybrid amorphous miscible LA-CL became richer in CL and, as a result, the T_{g1} takes lower values.

As the major changes were found on the first day, the microstructure of PLCL_{r1} after being submerged in PBS during this time was analyzed by means of AFM. Figure 7 shows the height and phase images (a-b), as well as their corresponding 3D images (c-d). Referring to height image, the presence of small spherulites (< 5 μm) within the copolymer can easily be seen. This evidence proves that crystals are formed during aging, which is in accordance with the results observed in the DSC. Regarding the phase images, two different regions are clearly observed; on the one hand, a crystalline matrix (in brown) and on the other, white isolated domains typically located on the exterior of the spherulites. On the basis of the DSC results, the crystalline structure should be ascribed to PLLA crystals, while the second dispersed phase to the amorphous phase of polylactide prompted by the crystallization of lactide building blocks during aging. Therefore, the microstructure of PLCL_{r1} after being submerged for 1 day in PBS can be described as a three phase model structure consisting of a hybrid miscible LA-CL amorphous phase, PLLA crystals and a constrained PLLA amorphous phase located in the immediate vicinity of the crystals.

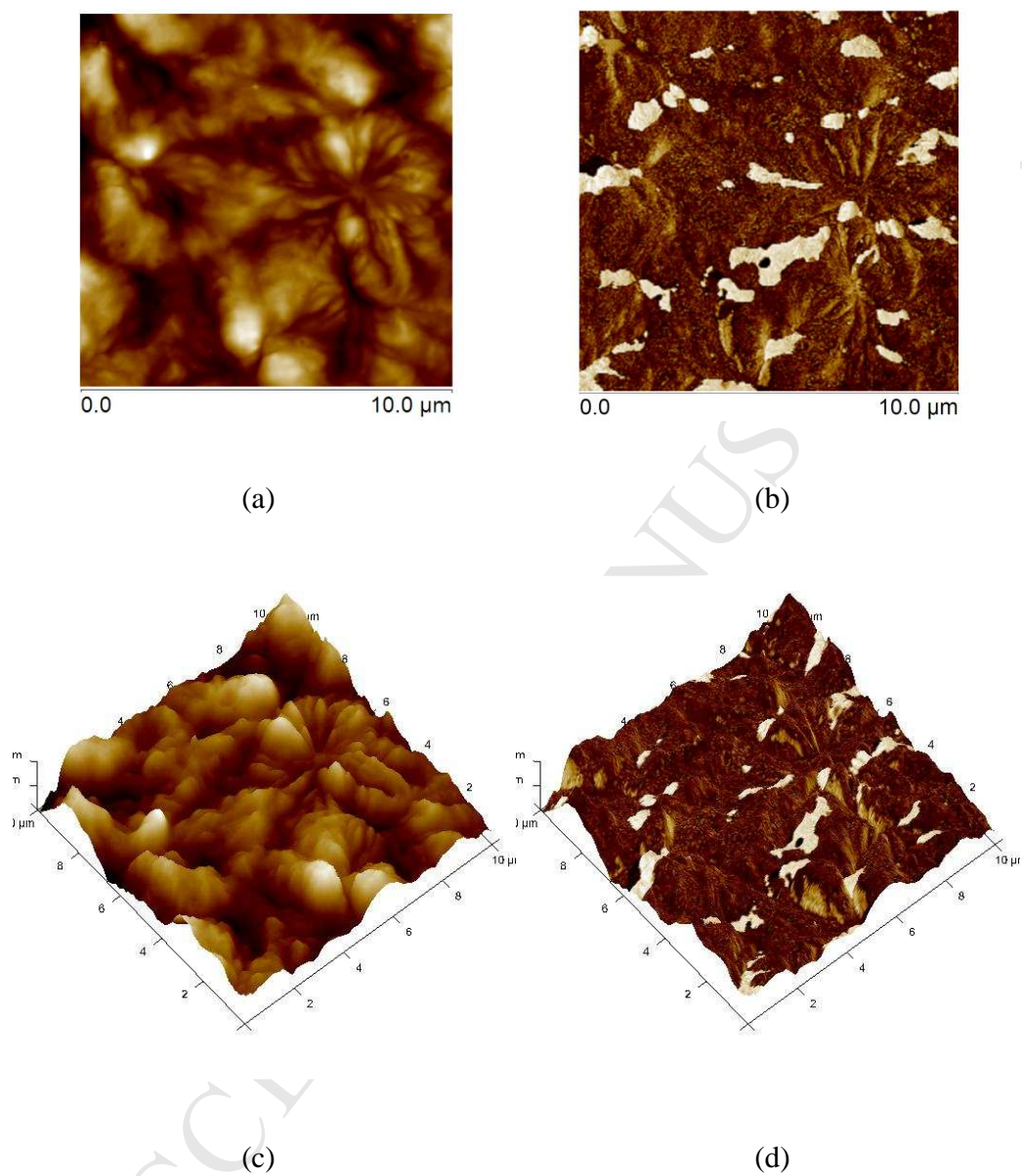


Figure 7. AFM images of PLCL_{r1} after being submerged in PBS for 1 day (a) height image (b) phase image (c) 3D height image (d) 3D phase image.

The immobilization of the PLLA amorphous phase between crystals; hence the reduction in segmental mobility might be the responsible for the shift of T_{g2} towards the high-temperature side with t_a . T_{g2} increases by almost 9 °C after one week, suggesting that a more constrained PLLA amorphous phase is formed during aging.

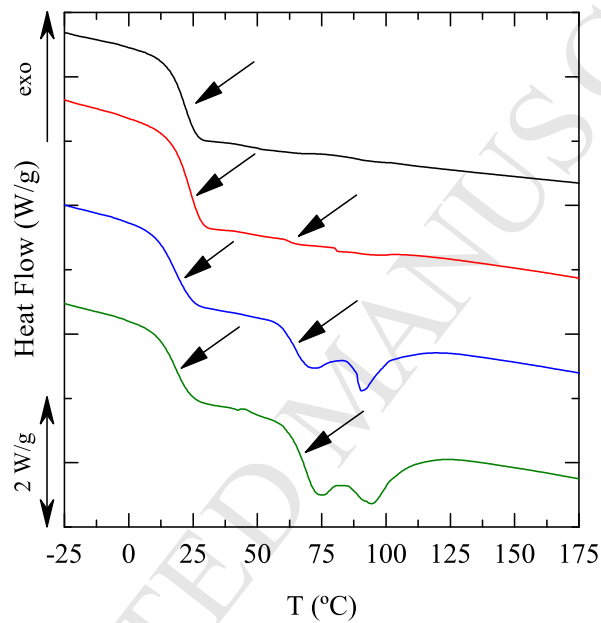


Figure 8. First DSC scans for PLCLr₂ samples submerged in PBS at 37 °C during 0 (black), 1 (red), 3 (blue) and 7 (green) days.

A similar evolution is found for PLCLr₂, Figure 8, as it shows double T_g behavior but the second T_g appears on day 3 instead of on day 1. The melting temperature for PLCLr₂ was found to be lower than for PLCLr₁, at ~ 91 °C. The ΔH_m value also seems to be smaller than that found for

PLCL_{r1}. However, the overlapping signals of T_{g2} transition and melting makes the measurements of ΔH_m difficult.

In view of these results, it can be concluded that the different chain microstructures of the studied PLCLs directly affect the chain rearrangements occurring during their storage in PBS at 37 °C. PLCL_{r1}, which shows a longer L-lactide average sequence length in regard to PLCL_{r2} ($l_{LA}=4.35$ vs. 3.45), crystallized faster and the associated phase separation occurs earlier than in PLCL_{r2}.

Figure 9 shows the DMA results for PLCL_{r1} submerged in PBS at 0, 1, 3 and 7 days. The values of $\tan \delta$, the temperature of E' onset ($T_{E' \text{ onset}}$) are summarized in Table 6. T_{onset} was calculated as the point where the initial E' value departs from linearity.

Tan δ curves show a single transition with a maximum value of 1.6 centered at ~32 °C on day 0. After only 1 day submerged in PBS, the value of $\tan \delta$ decreased to ~0.5 and shifted to lower temperatures, indicating a reduction in the sample's amorphous fraction and the increase in CL in the amorphous phase content due to the migration of LA sequences from the amorphous hybrid phase to the polylactide crystalline domains. However, in contrast to the single transition observed in $\tan \delta$ curves, two different transitions are discernible in E' curves for aged samples. A single fall is observed for the sample on day 0, while for samples submerged in PBS two different falls in E' are observed. This could indicate the existence of two different phases. The second transition around 65 °C is in good agreement with the values registered for T_{g2} by DSC. (see

Table 5). Moreover, $T_{E' \text{ onset}}$ shifts to a lower temperature with t_a , indicating that a lower temperature is required for the first transition. This means that the value of T_{g1} should be lower with aging, which was confirmed by the DSC results.

Moreover, the value of E' after the second transition remained quite high, between 60-100 MPa, indicating that the lactide crystals formed during aging contribute to the maintenance of storage modulus of the material.

Table 6. DMA properties of $PLCLr_1$ and $PLCLr_2$ after conformation by melt-quenching (0 day) in water and after being submerged in PBS for 1, 3 and 7 days. $T_{\tan\delta}$: temperature at which $\tan\delta$ is maximum; $\tan\delta$: value of the $\tan\delta$ peak and $T_{E' \text{ onset}}$: the temperature where the initial value of E' departs from linearity.

		$T_{\tan\delta}$ (°C)	$\tan\delta$ (value)	$T_{E' \text{ onset}}$ (°C)
$PLCLr_1$	0	31.6	1.7	7.66
	1	27.2	0.45	2.28
	3	22.7	0.36	-3.36
	7	22.7	0.36	-1.77
$PLCLr_2$	0	30.4	2.1	10.9
	1	31.36	1.99	10.05
	3	27.47	0.84	7.94
	7	25.7	0.61	6.7

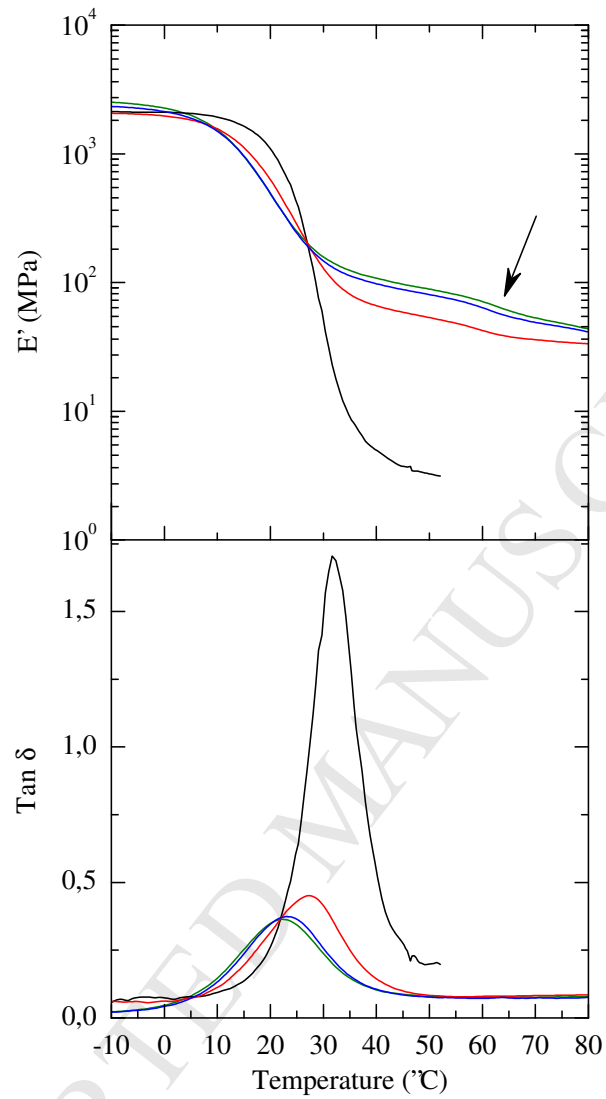


Figure 9. Storage modulus (above) and $\tan \delta$ (below) of PLCL r_1 submerged in PBS at 37 °C during 0 (black), 1 (red), 3 (blue) and 7 (green) days.

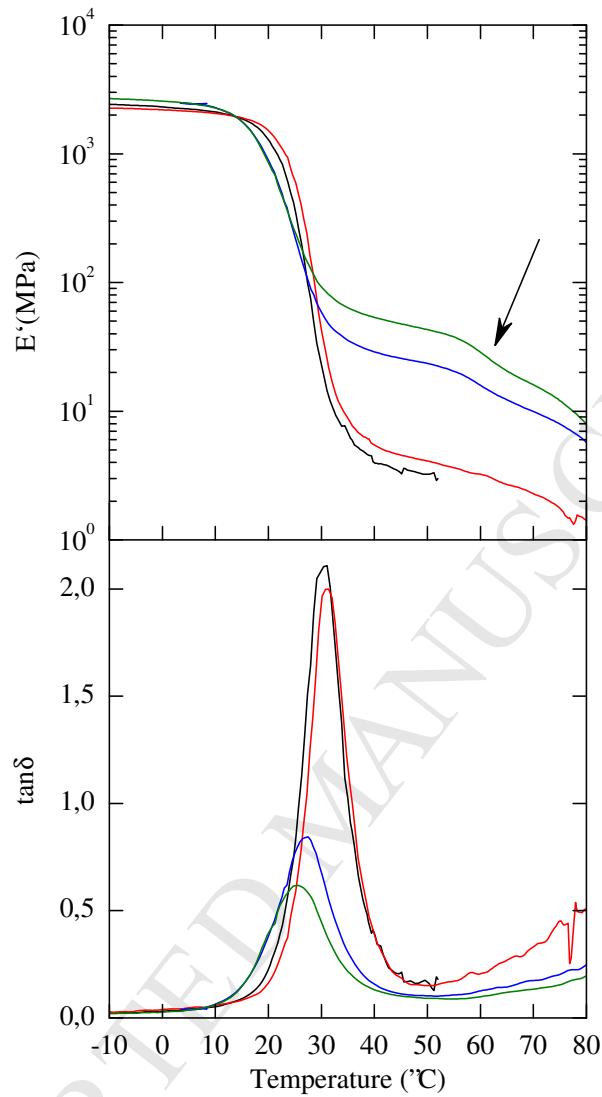


Figure 10. Storage modulus (above) and $\tan \delta$ (below) of PLCL r_2 submerged in PBS at 37 °C during 0 (black), 1 (red), 3 (blue) and 7 (green) days.

An analysis of the DMA results shows that similar behavior was observed for PLCL r_2 after being submerged in PBS at 0, 1, 3 and 7 days. DMA curves are illustrated in Figure 10.

In this case, in contrast to PLCL_{r1}, the main changes are observed after 3 days submerged in PBS. On day 3, the tan δ maximum fell from ~ 2.0 to ~ 0.8 and finally to 0.6 due to the migration of LA units to the crystalline region and moved toward lower temperatures. Moreover, it was observed that $T_{E'_{\text{onset}}}$ shifts towards lower values with t_a , as in PLCL_{r1}. The second transition, associated with T_{g2} is observed around 60 °C on day 3 and 7 which is in agreement with the DSC data, Figure 8.

Although the behavior of both copolymers, PLCL_{r1} and PLCL_{r2}, are similar, some differences are worth mentioning. The rate at which the $T_{E'_{\text{onset}}}$ shifts toward lower temperatures is much slower for PLCL_{r2} than for PLCL_{r1}. This means that chain rearrangements of lactide sequences into defined spherulites is delayed for copolymers with a higher randomness character making crystal formation more difficult. Moreover, if the values of tan δ for both copolymers are compared, it can easily be seen that in all cases higher values are reported for PLCL_{r2} indicating a higher content of the amorphous phase. This fact is consistent with the results observed for $T_{E'_{\text{onset}}}$. The early melting peak detected for PLCL_{r2} in comparison to PLCL_{r1} in the DSC traces, Figure 8, is also corroborated by DMA results. For this copolymer, after the second fall in E' curves a second fall is observed around 80 °C, which is associated with the melting of the lactide sequence block crystals. A comparison of these curves for both copolymers at this temperature, ~ 80 °C, shows a difference. While the E' values at 80 °C ranges from 33 to 44 MPa for PLCL_{r1}, the values for PLCL_{r2} range from 5.5 to 8 MPa. Crystals within PLCL_{r1} melt at higher temperature, and therefore PLCL_{r1} keeps higher values of E' after T_{g2} over the same temperature range.

CONCLUSIONS

The relaxation behavior and the phase structural changes of PLLA, PDLLA, and two PLCLs with different randomness character were studied after being subjected to a physical aging process at 37 °C in PBS.

For PLLA and PDLLA, TMDSC was regarded as a valuable extension of conventional DSC, and was particularly beneficial for the individual evaluation of the change in C_p and relaxation enthalpy signals of aged samples.

The main conclusions of this works are the following:

- The polymers studied present molecular rearrangements after being submerged at 37 °C in PBS for only 1 day.
- PLLA and PDLLA, underwent a physical aging process during the course of the experiment. The increase in the value of δ observed by TMDSC and the narrowing of the $\tan\delta$ peak in DMA indicated the reduction in molecular mobility and a more uniform distribution of the entropic states as the time submerged in PBS increased.
- PLLA samples aged for longer times are more prone to crystallize upon heating, as demonstrated by the increase in ΔH_c and the increase of E' in the DMA curves. Therefore, it can be concluded that aging is a precursor of the cold crystallization process.
- PLLA showed a higher potential to reach the equilibrium compared to PDLLA.
- $PLCL_{r_1}$ and $PLCL_{r_2}$ suffered important supramolecular arrangements, which were clearly affected by the initial l_{LA} . In both cases, the formation of PLLA crystals was accompanied by a phase separation of the initially single phase copolymer. The two T_g s

found in the DSC traces, the two E' drops observed in DMA as well as the phase images achieved by AFM corroborated this phase behavior.

- Crystalline domains appeared in PLCL r_1 after only 1 day submerged in PBS, whereas in PLCL r_2 it took 3 days. The presence of the lactide block crystals revealed themselves as a melting peak in the DSC scans and also in the reduction of $\tan\delta$ observed by DMA.
- Due to the more random character, PLCL r_2 showed slower microstructural changes as well as a lower propensity to crystallize, which led to less stable crystals with lower T_m in comparison to PLCL r_1 .

REFERENCES

1. Hutchinson JM. Relaxation processes and physical aging. In: The Physics of Glassy Polymers, Haward RN, Young RJ, editors. London: Chapman and Hall, 1997. p. 85.
2. Reading M, Hourston DJ, Editors. Modulated Temperature Differential Scanning Calorimetry: Theoretical and Practical Applications in Polymer Characterisation. Dordrecht: Kluwer Academic Publishers, 2006.
3. Schick C. Temperature modulated differential scanning calorimetry (TMDSC) - basics and applications to polymers. Handb Therm Anal Calorim 2002;3:713-810.
4. Wunderlich B, Editor. Thermal Analysis of Polymeric Materials. Berlin: Springer-Verlag, 2005.
5. Pyda M, Wunderlich B. Reversing and Nonreversing Heat Capacity of Poly(lactic acid) in the Glass Transition Region by TMDSC. Macromolecules 2005;38(25):10472-10479.

6. Trotignon J, Verdu J, Dobracginsky A. Comportement à long terme. In: *Matières Plastiques: Structures-Propriétés*, Paris: Nathan, 1996. p. 46.
7. Verdu J. *Plastics. Long-term behavior*. *Tech Ing , Gen* 1976;29(A78):19-52.
8. Kurtz SM, Pruitt LA, Crane DJ, Edidin AA. Evolution of morphology in UHMWPE following accelerated aging: The effect of heating rates. *J Biomed Mater Res* 1999;46:112-120.
9. Foster SP, Spohn WW. Accelerated heat aging of polyethylene. *Wire Wire Prod* 1955;30:1487.
10. Bhateja SK. Changes in the crystalline content of irradiated linear polyethylenes upon ageing. *Polymer* 1982;23:654-655.
11. Wang Y, Mano JF. Effect of structural relaxation at physiological temperature on the mechanical property of poly(L-lactic acid) studied by microhardness measurements. *J Appl Polym Sci* 2006;100(4):2628-2633.
12. Liao K, Quan D, Lu Z. Effects of physical aging on glass transition behavior of poly(-lactide). *Eur. Polym. J.* 2002;38(1):157-162.
13. Kwon M, Lee SC, Jeong YG. Influences of physical aging on enthalpy relaxation behavior, gas permeability, and dynamic mechanical property of polylactide films with various D-isomer contents. *Macromol Res* 2010;18(4):346-351.
14. Pan P, Zhu B, Dong T, Yazawa K, Shimizu T, Tansho M, Inoue Y. Conformational and microstructural characteristics of poly(L-lactide) during glass transition and physical aging. *J Chem Phys* 2008;129(18):184902/1-184902/10.

15. Pan P, Zhu B, Inoue Y. Enthalpy Relaxation and Embrittlement of Poly(L-lactide) during Physical Aging. *Macromolecules* 2007;40(26):9664-9671.
16. Pan P, Liang Z, Zhu B, Dong T, Inoue Y. Roles of Physical Aging on Crystallization Kinetics and Induction Period of Poly(L-lactide). *Macromolecules* 2008;41(21):8011-8019.
17. Saha SK, Tsuji H. Enhanced crystallization of poly(L-lactide-co-ε-caprolactone) in the presence of water. *J Appl Polym Sci* 2009;112(2):715-720.
18. Tsuji H, Mizuno A, Ikada Y. Enhanced crystallization of poly(L-lactide-co-ε-caprolactone) during storage at room temperature. *J Appl Polym Sci* 2000;76(6):947-953.
19. Jone MU, Sarasua JR. Effect of aging on mechanical behavior of a biodegradable poly(lactide-caprolactone) copolymer. ANTEC 2011-Proceedings of the 69th Annual Technical Conference & Exhibition 2011:1964-1968.
20. Fernández J, Etxeberria A, Ugartemendia JM, Petisco S, Sarasua J. Effects of chain microstructures on mechanical behavior and aging of a poly(L-lactide-co-ε-caprolactone) biomedical thermoplastic-elastomer. *J. Mech. Behav. Biomed. Mater.* 2012;12(0):29.
21. Na B, Zou S, Lv R, Luo M, Pan H, Yin Q. Unusual Cold Crystallization Behavior in Physically Aged Poly(L-lactide). *J Phys Chem B* 2011;115(37):10844-10848.
22. Struik LCE. The mechanical and physical aging of semicrystalline polymers. 1. *Polymer* 1987;28(9):1521-1533.
23. Struik LCE. The mechanical behavior and physical aging of semicrystalline polymers. 2. *Polymer* 1987;28(9):1534-1542.

24. Wang Y, Ribelles JLG, Sanchez MS, Mano JF. Morphological Contributions to Glass Transition in Poly(L-lactic acid). *Macromolecules* 2005;38(11):4712-4718.

25. Fox TG. Influence of diluent and of copolymer composition on the glass temperature of a polymer system. *Bull Am Phys Soc* [2] 1956;1:123.

ACKNOWLEDGMENT

The authors are thankful for funds of the Basque Government (GV/EJ), Department of Education, Universities and Research (GIC10/152-IT-334-10) and Dept. of Industry (IE10/276), MICINN (BIO2010-21542-C02-01), and for the pre-doctoral grant from GV/EJ for J. M. U. The authors thank also the University of the Basque Country (UPV-EHU) for a pre-doctoral grant for A.L.E and H.A.M.